Weak localization of the open kicked rotator

J. Tworzydło,[1,2] A. Tajic,[1] and C. W. J. Beenakker[1]
[1]*Instituut-Lorentz, Universiteit Leiden, P.O. Box 9506, 2300 RA Leiden, The Netherlands*
[2]*Institute of Theoretical Physics, Warsaw University, Hoża 69, 00-681 Warsaw, Poland*
(Received 6 May 2004; published 17 November 2004)

We present a numerical calculation of the weak localization peak in the magnetoconductance for a stroboscopic model of a chaotic quantum dot. The magnitude of the peak is close to the universal prediction of random-matrix theory. The width depends on the classical dynamics, but this dependence can be accounted for by a single parameter: the level curvature around zero magnetic field of the closed system.

DOI: 10.1103/PhysRevB.70.205324 PACS number(s): 73.20.Fz, 73.63.Kv, 05.45.Mt, 05.45.Pq

I. INTRODUCTION

Random-matrix theory (RMT) makes system-independent ("universal") predictions about quantum-mechanical systems with a chaotic classical dynamics.[1–4] The presence or absence of time-reversal symmetry (TRS) identifies two universality classes. RMT is also capable of describing the crossover between the universality classes, e.g., when TRS is broken by the application of a magnetic field B. The crossover is predicted to depend on a single system-specific parameter, namely, the mean absolute curvature of the energy levels E_i around $B=0$. More precisely, a universal magnetic-field dependence of spectral correlations is predicted when B is rescaled by the characteristic field

$$B_c = \left(\frac{1}{\Delta} \left\langle \left| \frac{d^2 E_i}{dB^2} \right|_{B=0} \right\rangle \right)^{-1/2}, \tag{1.1}$$

with Δ the mean level spacing. This prediction has been tested in a variety of computer simulations.[5–7]

In open systems a similar prediction of universality for transport properties exists, but now the characteristic field also depends on the conductance g of the point contacts that couple the chaotic quantum dot to electron reservoirs.[8–11] A universal magnetic field dependence is predicted if B is rescaled by $B_c\sqrt{g}$, provided g is large compared to the conductance quantum e^2/h. To provide a numerical test of this prediction is the purpose of this paper.

We present a computer simulation of the open quantum kicked rotator,[12–15] which is a stroboscopic model of a quantum dot coupled to electron reservoirs by ballistic point contacts. The ensemble averaged conductance increases upon breaking of TRS, as a manifestation of weak localization. The height, width, and line shape of the weak localization peak are compared with the predictions of RMT.

The simulation itself is straightforward, but the formulation of the model is not. There exist several ways to break TRS in the closed kicked rotator[16–19] and related models.[20–23] When opening up the system one needs to ensure that the scattering matrix satisfies the reciprocity relation

$$S(-B) = S^T(B), \tag{1.2}$$

which holds under the assumption that the electrostatic potential is B independent. (The superscript T indicates the transpose of the scattering matrix S.) We also require that TRS is broken already at the level of the classical dynamics (as it is in a quantum dot in a uniform magnetic field). Finally, we need to relate the TRS-breaking parameter in the stroboscopic formulation to the flux enclosed by the quantum dot. All these issues are addressed in Secs. II and III before we proceed to the actual simulation in Sec. IV. We conclude in Sec. V.

II. TIME-REVERSAL-SYMMETRY BREAKING IN THE OPEN KICKED ROTATOR

A. Formulation of the model

The kicked rotator is a particle moving along a circle, kicked periodically at time intervals τ_0.[1,17] The stroboscopic time evolution of a wave function is given by the Floquet operator $\mathcal{F}$. In addition to the stroboscopic time τ_0 and the moment of inertia I, which we set to unity, F depends on the kicking strength K and the TRS-breaking parameter γ. We require

$$\mathcal{F}(-\gamma) = \mathcal{F}^T(\gamma), \tag{2.1}$$

which guarantees the reciprocity relation (1.2) for the scattering matrix when we open up the model.

We will consider two different representations of $\mathcal{F}$, both of which can be written as an $M\times M$ unitary matrix. The classical limit corresponds to a map defined on a toroidal phase space. The difference between the two representations is whether TRS breaking persists in the classical limit or not. The simplest representation of $\mathcal{F}$ has one kick per period. It breaks TRS quantum mechanically, but not classically. This would correspond to a quantum dot that encloses a flux tube, but in which the magnetic field vanishes. A more realistic model has TRS breaking both at the quantum mechanical and at the classical level. We have found that we then need a minimum of three kicks per period.

B. Three-kick representation

We will mainly consider the three-kick model, so we describe it first. In this model TRS is broken both quantum mechanically and classically. Stroboscopic models with multiple kicks per period of different magnitude were studied previously in the context of quantum rachets.[21] Inspired by that work, we study the time-dependent Hamiltonian

 ©2004 The American Physical Society

$$H(t) = \frac{p^2}{2} + \frac{1}{2}V(\theta)\sum_n [\delta_\epsilon(t-n+\epsilon) + \delta_\epsilon(t-n-\epsilon)] + \gamma\cos(\theta)\sum_n \delta(t-n+1/3) - \gamma\cos(\theta)\sum_n \delta(t-n-1/3), \tag{2.2}$$

with ϵ an infinitesimal. The angular momentum operator $p=-i\hbar_{\rm eff}\partial_\theta$ is canonically conjugate to the angle $\theta\in[0,2\pi)$. The effective Planck constant is $\hbar_{\rm eff}=\hbar\tau_0/I$. The potential[18,19,24,25]

$$V(\theta) = K\cos(\pi q/2)\cos(\theta) + \tfrac{1}{2}K\sin(\pi q/2)\sin(2\theta) \tag{2.3}$$

with $q\neq 0$ breaks the parity symmetry of the model. The form of the potential is such that in the large K limit the diffusion constant does not depend on q. For $\gamma=0$ there are two kicks per period in Eq. (2.2), but since they are displaced by an infinitesimal amount we still call this a "single-kick" model. For $\gamma\neq 0$ two more kicks appear with opposite sign at finite displacement. We will see that this choice guarantees the reciprocity criterion (2.1) for the Floquet operator.

The reduction of the Floquet operator

$$\mathcal{F} = \mathcal{T}\exp\left[-\frac{i}{\hbar_{\rm eff}}\int_0^1 H(t)dt\right] \tag{2.4}$$

(with $\mathcal{T}$ the time ordering operator) to a discrete, finite form is obtained only for special values of $\hbar_{\rm eff}$, known as resonances.[17] We have to reconsider the usual condition for resonances in the presence of additional, TRS-breaking kicks. Here our analysis departs from the quantum rachet analogy.[21]

The initial wave function $\psi(\theta)$ evolves in one period to a final wave function $\overline{\psi}(\theta)$, given by

$$\overline{\psi}(\theta) = \exp[-iV(\theta)/2\hbar_{\rm eff}]\exp(i\hbar_{\rm eff}\partial_\theta^2/6) \times\exp[-i\gamma\cos(\theta)/\hbar_{\rm eff}]\exp(i\hbar_{\rm eff}\partial_\theta^2/6) \times\exp[i\gamma\cos(\theta)/\hbar_{\rm eff}]\exp(i\hbar_{\rm eff}\partial_\theta^2/6) \times\exp[-iV(\theta)/2\hbar_{\rm eff}]\psi(\theta). \tag{2.5}$$

One recognizes three factors describing free propagation for $1/3$ of a period, each followed by a kick. The resonance condition for free propagation is $\hbar_{\rm eff}=2\pi r/M$, with r an odd integer and M an even integer.[17] The free propagation

$$\psi_1(\theta) = \exp(i\hbar_{\rm eff}\partial_\theta^2/6)\psi(\theta) \tag{2.6}$$

is then given by

$$\psi_1\left(\theta+\frac{2\pi}{3M}n\right) = \frac{1}{3M}\sum_{m,n'=0}^{3M-1}\exp\left(-i\frac{2\pi r}{3M}m^2\right) \times\exp\left(-im\frac{2\pi}{3M}(n'-n)\right)\psi\left(\theta+\frac{2\pi}{3M}n'\right). \tag{2.7}$$

Resonance means that the initial and final wave functions can be treated as discrete vectors on a $3M$-point lattice, labeled by the indices n,n'. The angle θ is an arbitrary offset parameter. Different values of θ are not coupled by the free propagation. Putting together three iterations of Eq. (2.7) we get three independent components of $\psi(\theta+2\pi n/3M)$ for $n=0,1,2$ (mod 3), each on an M-point lattice.

We find that the resonance property is preserved in the presence of intervening TRS-breaking kicks, provided that $r=3$ and M even, but not a multiple of 3. The free propagation (2.7) then is conveniently expressed in matrix notation. The matrix acts on an M-component vector $\psi_m=\psi(\theta+2\pi m/3M)$, $m=0,\ldots,M-1$. We choose the arbitrary phase $\theta=0$, so that

$$(\psi_1)_m = \sum_{m'=0}^{M-1}(U^\dagger\Sigma U)_{mm'}\psi_{m'}. \tag{2.8}$$

The matrices are defined by

$$\Sigma_{mm'} = \delta_{mm'}e^{-i\pi m^2/M}, \tag{2.9}$$

$$U_{mm'} = M^{-1/2}e^{-2\pi imm'/M}. \tag{2.10}$$

The matrix product $U^\dagger\Sigma U$ can be evaluated in closed form, with the result

$$\Pi_{mm'} = (U^\dagger\Sigma U)_{mm'} = M^{-1/2}e^{-i\pi/4}\exp[i(\pi/M)(m'-m)^2]. \tag{2.11}$$

Collecting results, we find that for $\hbar_{\rm eff}=6\pi/M$ the Floquet operator (2.5) is represented by an $M\times M$ unitary matrix, of the form

$$\mathcal{F}_{mm'} = (X\Pi Y^*\Pi Y\Pi X)_{mm'}, \tag{2.12a}$$

$$Y_{mm'} = \delta_{mm'}e^{i(M\gamma/6\pi)\cos(2\pi m/M)}, \tag{2.12b}$$

$$X_{mm'} = \delta_{mm'}e^{-i(M/12\pi)V(2\pi m/M)}. \tag{2.12c}$$

One readily verifies the reciprocity relation (2.1).

The classical map corresponding to this quantum mechanical model is derived in Appendix A. We show there that TRS breaking of the classical map is broken for $\gamma\neq 0$ in the three-kick model.

C. One-kick representation

TRS breaking in the one-kick model is constructed as a formal analogy to the magnetic vector potential, by adding an offset δ to the momentum of the kicked rotator.[16–19,24–26] To obey reciprocity

$$\mathcal{F}(-\delta) = \mathcal{F}^T(\delta) \tag{2.13}$$

for odd M it is enough to symmetrize the expression of Ref. 16 by infinitesimally splitting the kick (as it was done in Ref. 15 for $\delta=0$). For even M, which is more convenient for application of the fast Fourier transform, one also needs to redefine the lattice points in order to preserve reciprocity.[27]

The model takes the form

$$\mathcal{F}_{mm'} = (\tilde{X}\tilde{U}^{\dagger}\tilde{\Pi}\tilde{U}\tilde{X})_{mm'}, \tag{2.14a}$$

$$\tilde{U}_{mm'} = M^{-1/2} e^{-2\pi i[m-(M-1)/2]m'/M}, \tag{2.14b}$$

$$\tilde{X}_{mm'} = \delta_{mm'} e^{-i(MK/4\pi)\cos(2\pi m/M+\phi)}, \tag{2.14c}$$

$$\tilde{\Pi}_{mm'} = \delta_{mm'} e^{-i\pi[m-(M-1)/2-\delta(M/2\pi)]^2/M}. \tag{2.14d}$$

In addition to the TRS-breaking phase δ there is a phase ϕ to break the parity symmetry. The reciprocity property (2.13) can easily be checked.

The classical map corresponding to this model is also discussed in Appendix A. It does not break TRS.

D. Scattering matrix

To model a pair of N-mode ballistic point contacts that couple the quantum dot to electron reservoirs, we impose open boundary conditions in a subspace of Hilbert space represented by the indices $m_n^{(\alpha)}$. The subscript $n=1,2,\ldots,N$ labels the modes and the superscript $\alpha=1,2$ labels the leads. A $2N\times M$ projection matrix P describes the coupling to the ballistic leads. Its elements are

$$P_{nm} = \begin{cases} 1 & \text{if } m=n\in\{m_n^{(\alpha)}\}, \\ 0 & \text{otherwise.} \end{cases} \tag{2.15}$$

The mean dwell time is $\tau_D = M/2N$ (in units of τ_0).

The matrices P and $\mathcal{F}$ together determine the scattering matrix[13–15]

$$S(\varepsilon) = P[e^{-i\varepsilon} - \mathcal{F}(1-P^TP)]^{-1}\mathcal{F}P^T, \tag{2.16}$$

where ε is the quasienergy. The reciprocity condition (2.1) of $\mathcal{F}$ implies that also S satisfies the reciprocity condition (1.2).

By grouping together the N indices belonging to the same point contact, the $2N\times 2N$ matrix S can be decomposed into 4 sub-blocks containing the $N\times N$ transmission and reflection matrices

$$S = \begin{pmatrix} r & t \\ t' & r' \end{pmatrix}. \tag{2.17}$$

The conductance G (in units of e^2/h, disregarding spin degeneracy) follows from the Landauer formula

$$G = \mathrm{Tr}\, tt^{\dagger}. \tag{2.18}$$

III. RELATION WITH RANDOM-MATRIX THEORY

In RMT time-reversal symmetry is broken by means of the Pandey-Mehta Hamiltonian[28]

$$H = H_0 + i\alpha A, \tag{3.1}$$

which consists of the sum of a real symmetric matrix H_0 and a real antisymmetric matrix A with imaginary weight $i\alpha$. We denote by M_H the dimensionality of the Hamiltonian matrix. The two matrices H_0 and A are independently distributed with the same Gaussian distribution. The variance $\nu^2 = \langle (H_0)_{ij}^2\rangle = \langle A_{ij}^2\rangle$ $(i\neq j)$ determines the mean level spacing $\Delta = \pi\nu/\sqrt{M_H}$ at the center of the spectrum for $M_H \gg 1$ and $\alpha \ll 1$.

To lowest order in perturbation theory the energy levels $E_i(\alpha)$ depend on the TRS-breaking parameter α according to

$$\delta E_i = \alpha^2 \sum_{j\neq i} \frac{A_{ij}^2}{E_i - E_j}, \tag{3.2}$$

with $\delta E_i = E_i(\alpha) - E_i(0)$ and $E_i \equiv E_i(0)$. The characteristic value α_c is determined by the mean absolute curvature

$$\alpha_c \equiv \left(\frac{1}{\Delta} \left\langle \left| \frac{d^2E_i}{d\alpha^2}\right|_{\alpha=0} \right\rangle \right)^{-1/2}. \tag{3.3}$$

From Eq. (3.2) we deduce that $\alpha_c \simeq \Delta/\nu \simeq 1/\sqrt{M_H}$, up to a numerical coefficient of order unity. A numerical calculation gives

$$\alpha_c \sqrt{M_H} \equiv \kappa_{\mathrm{RMT}} = 1.27. \tag{3.4}$$

A real magnetic field B is related to the parameter α of RMT by

$$B/B_c = \alpha/\alpha_c, \tag{3.5}$$

where B_c is determined by the level curvature according to Eq. (1.1). For a ballistic two-dimensional billiard (area A, Fermi velocity v_F) with a chaotic classical dynamics, one has[2,5]

$$B_c = c\frac{h}{eA}(\Delta\sqrt{A}/\hbar v_F)^{1/2}, \tag{3.6}$$

with c a numerical coefficient that depends only on the shape of the billiard. The field B_c corresponds to a flux through the quantum dot of order $(h/e)\sqrt{\tau_{\mathrm{erg}}\Delta/\hbar} \ll h/e$, with the ergodic time τ_{erg} being the time it takes an electron to explore the available phase space in the quantum dot.

The analog of Eqs. (1.1) and (3.5) for the quantum kicked rotator considered here is

$$\gamma/\gamma_c = \alpha/\alpha_c, \quad \gamma_c \equiv \left(\frac{M}{2\pi} \left\langle \left| \frac{d^2\phi_i}{d\gamma^2}\right|_{\gamma=0} \right\rangle \right)^{-1/2}. \tag{3.7}$$

Here γ is the TRS-breaking parameter in the three-kick model. The same relation applies to the one-kick model, with γ,γ_c replaced by δ,δ_c.

To complete the correspondence between the kicked rotator, RMT, and the real quantum dot, we need to determine the two characteristic values γ_c and δ_c. In Appendix B we present an analytical calculation deep in the chaotic regime $(K\to\infty)$, according to which

$$\lim_{K\to\infty} \gamma_c = 12\pi M^{-3/2}\kappa_{\mathrm{RMT}} = 47.9\ M^{-3/2}, \tag{3.8}$$

$$\lim_{K\to\infty} \delta_c = 4\sqrt{3} M^{-3/2}\kappa_{\mathrm{RMT}} = 8.80\ M^{-3/2}. \tag{3.9}$$

In Figs. 1 and 2 we show a numerical calculation for finite K, which confirms these analytical large-K limits.

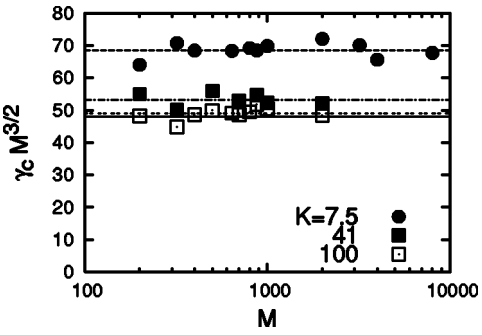

FIG. 1. The critical value γ_c of the TRS-breaking parameter in the closed three-kick model is presented for different system sizes at fixed K. The parity-breaking parameter is $q=0.2$. The solid line shows the large-K limit (3.8). The dashed lines are averages over M of the numerical data.

In the open system the characteristic field scale for TRS breaking is increased by a factor $\sqrt{g}$, with g the conductance of the point contacts. We consider ballistic N-mode point contacts, so that $g=N$, measured in units of e^2/h. The conductance $G(B)$ of the quantum dot is also measured in units of e^2/h. According to RMT, the weak localization magnetoconductance is given by[9,11]

$$G(B) = \frac{N}{2} - \frac{1}{4}[1 + (2\kappa_{\mathrm{RMT}} N^{-1/2} B/B_c)^2]^{-1}. \quad (3.10)$$

For the quantum kicked rotator we would therefore expect a weak localization peak in the conductance given by

$$G(\gamma) = G_\infty - \tfrac{1}{4}[1 + (2\kappa_{\mathrm{RMT}} N^{-1/2} \gamma/\gamma_c)^2]^{-1}, \quad (3.11)$$

in the three-kick model. We define the weak localization correction $\delta G(\gamma) = G(\gamma) - G_\infty$, with G_∞ the conductance at fully broken TRS. The expression in the one-kick model is similar, with γ/γ_c replaced by δ/δ_c.

In the large-K limit we can use the analytical expressions (3.8) and (3.9) for γ_c and δ_c to obtain

$$\lim_{K\to\infty} \delta G(\gamma) = -\tfrac{1}{4}[1 + (M^{3/2} N^{-1/2} \gamma/6\pi)^2]^{-1}, \quad (3.12)$$

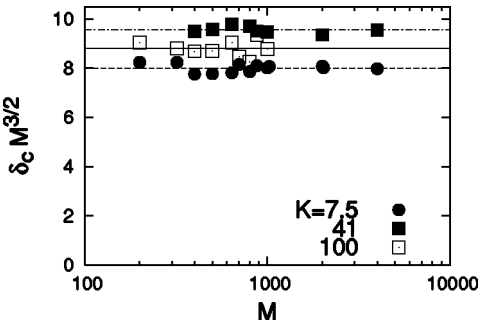

FIG. 2. Same as Fig. 1, but now for the closed one-kick model. The parity-breaking parameter is $\phi=0.2\pi$. The solid line shows the large-K limit (3.9).

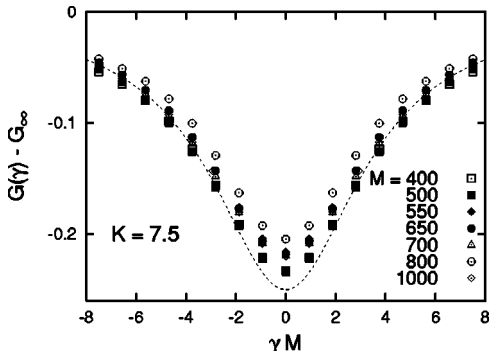

FIG. 3. Dependence of the average conductance on the TRS-breaking parameter γ. The three-kick model is characterized by $K=7.5$, $q=0.2$, and $\tau_D = M/2N = 25$. The dotted line shows the RMT prediction (3.11), with γ_c calculated from the mean level curvatures (Fig. 1).

$$\lim_{K\to\infty} \delta G(\delta) = -\tfrac{1}{4}[1 + (M^{3/2} N^{-1/2} \delta/2\sqrt{3})^2]^{-1}. \quad (3.13)$$

In Appendix C we show how these two results are consistent with a semiclassical calculation.

IV. NUMERICAL RESULTS

The numerical technique we use to calculate the conductance was described in Refs. 15 and 29. The calculation of the scattering matrix (2.16) is performed efficiently by use of an iterative procedure and the fast-Fourier-transform algorithm. We need to average over many system realizations (varying lead positions and quasienergies) to suppress statistical fluctuations. In addition, we need several points to plot the γ dependence. This makes the calculation for large M more time consuming than earlier studies of universal conductance fluctuations in the same model at zero magnetic field.[29,30]

First we present in Figs. 3 and 4 results for the weak localization correction δG in the three-kick model as a function of the TRS-breaking parameter γ. The data are obtained by averaging over 40 lead positions and 80 quasienergies. The parameter γ_c was calculated for the closed model using Eq. (3.7), and the resulting RMT prediction (3.11) is also shown (dotted curve).

To compare the simulation with RMT in more detail we have fitted a Lorentzian

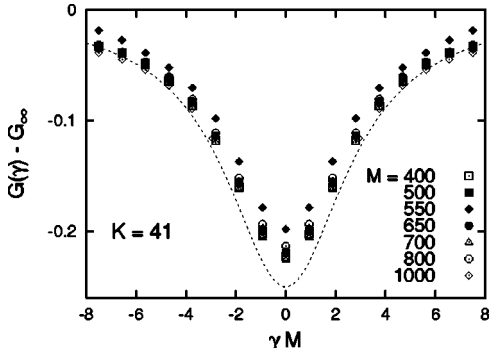

FIG. 4. Same as Fig. 3, but for $K=41$.

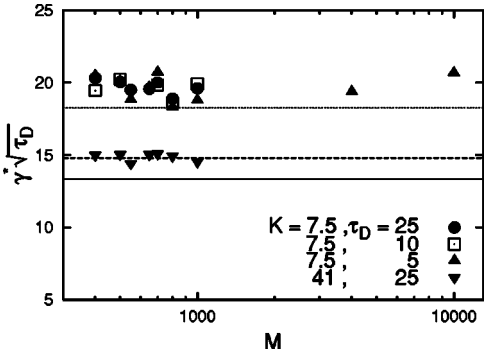

FIG. 5. Dependence of the crossover parameter γ^* on the system size. The data are obtained by fitting the Lorentzian (4.1) to the numerical data of Figs. 3 and 4. The solid line shows the large K limit (3.8). The dotted lines are the RMT prediction for $K=7.5$ and $K=41$, using γ_c found from the level curvatures in the closed model (Fig. 1).

$$\delta G = -\tfrac{1}{4}[1 + (M\gamma/\gamma^*)^2]^{-1} \tag{4.1}$$

to each data set. This is the RMT result (3.11) if $\gamma^* = \gamma^*_{\mathrm{RMT}} \equiv \gamma_c M^{3/2}/(2\sqrt{2\tau_D}\kappa_{\mathrm{RMT}})$. The large K limit is

$$\lim_{K\to\infty} \gamma^*_{\mathrm{RMT}} = 6\pi/\sqrt{2\tau_D}. \tag{4.2}$$

In Fig. 5 we plot the fitted crossover parameter γ^* as a function of M for fixed dwell time. The plot confirms the scaling with $\tau_D^{-1/2} \propto g^{-1/2}$, and also shows good agreement with the values of γ^*_{RMT} calculated from the mean level curvature (dotted lines).

We also performed numerical calculations for the one-kick model. The crossover scale δ^* extracted from a Lorentzian fit to the weak-localization peak was compared with the value $\delta^*_{\mathrm{RMT}} = \delta_c M^{3/2}/(2\sqrt{2\tau_D}\kappa_{\mathrm{RMT}})$ predicted by the mean level curvature. The large K limit of this value is

$$\lim_{K\to\infty} \delta^*_{\mathrm{RMT}} = \sqrt{6}/\sqrt{\tau_D}. \tag{4.3}$$

We show in Fig. 6 the ratio $\delta^*/\delta^*_{\mathrm{RMT}}$ for the one-kick model, as well as the ratio $\gamma^*/\gamma^*_{\mathrm{RMT}}$ for the three-kick model. The ratio is close to unity for both models if the dwell time is sufficiently large. At the smallest τ_D there is some deviation from unity in the one-kick model.

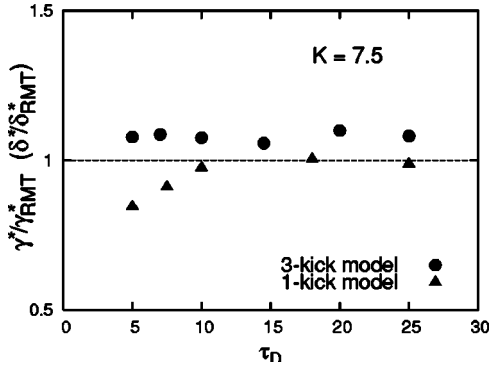

FIG. 6. Dependence of the ratio $\gamma^*/\gamma^*_{\mathrm{RMT}}$ for the three-kick model and the ratio $\delta^*/\delta^*_{\mathrm{RMT}}$ for the one-kick model on the dwell time τ_D. Data points for a given dwell time are obtained by averaging over system sizes in the range from 200 to 1000.

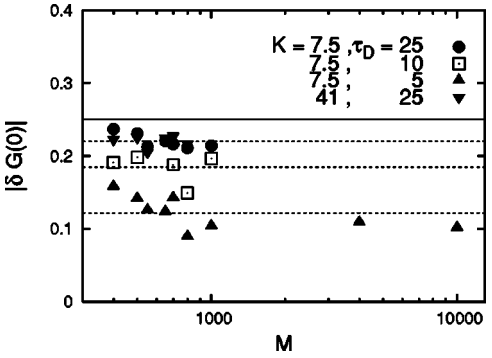

FIG. 7. Dependence of the amplitude of the weak localization peak $\delta G(0)$ (averaged over several system sizes) on the dwell time τ_D. Dashed lines show a linear dependence on $1/\tau_D$, extrapolated to the RMT value $|\delta G(0)| = 1/4$.

The magnitude of the weak localization peak in Figs. 3 and 4 shows a small (about 10%) discrepancy with the RMT prediction. We attribute this to nonergodic, short-time trajectories. We show in Fig. 7 the dependence of the magnitude of the weak localization peak $\delta G(0)$ on the dwell time. The results suggest that $\delta G(0) + \frac{1}{4} \propto 1/\tau_D$, a deviation from RMT to be expected from the Thouless energy scale (which is $\propto 1/\tau_D$). The deviation from unity in Fig. 6 has presumably the same origin.

We could determine the M dependence of γ^* and $\delta G(0)$ up to $M=10^4$ (for $K=7.5$ and $\tau_D=5$). The motivation for extending the calculation to large system sizes is to search for effects of the Ehrenfest time.[32,33] Although the Ehrenfest time $\tau_E \approx 3.8$ (estimating as in Ref. 15) was comparable to $\tau_D=5$, we did not find any systematic M-dependence in γ^* or $\delta G(0)$, cf. Figs. 5 and 8.

V. CONCLUSIONS

In conclusion, we have studied time-reversal symmetry breaking in quantum chaos through its effect on weak localization. We have found an overall good agreement between the universal predictions of random-matrix theory and the

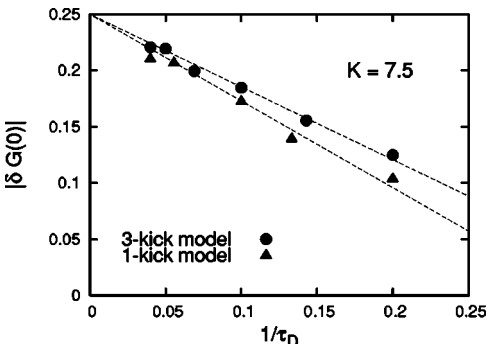

FIG. 8. Dependence of $\delta G(0)$ on the system size M for several dwell times. Dashed lines show averages over system size.

results for a specific quantum-mechanical model of a chaotic quantum dot. In particular, the scaling $\propto g^{-1/2}$ of the crossover magnetic field with the point contact conductance g is confirmed over a broad parameter range.

Deviations from RMT that we have observed scale inversely proportional with the mean dwell time τ_D, consistent with an explanation in terms of non-ergodic short-time trajectories. These deviations therefore have a classical origin.

More interesting deviations of a quantum mechanical origin have been predicted[32,33] in relation with the finite Ehrenfest time τ_E. This is the time scale on which a wave packet of minimal initial dimension spreads to cover the entire available phase space. The theoretical prediction is that the weak localization peak $\delta G(0) \propto e^{-\tau_E/\tau_D}$ should decay exponentially once τ_E exceeds τ_D. Our simulation extends up to $\tau_E \simeq \tau_D$, but shows no sign of this predicted decay. This is consistent with the explanation advanced by Jacquod and Sukhorukov[30] for the insensitivity of universal conductance fluctuations to a finite Ehrenfest time, based on the effective RMT of Ref. 31. As pointed out in Ref. 29, the same effective RMT also implies that weak localization should not depend on the relative magnitude of τ_E and τ_D.

Because our simulation could not be extended to the regime $\tau_E > \tau_D$, this final conclusion remains tentative. It might be that the exponential suppression of $\delta G(0)$ does exist, but that our system was simply too small to see it.

ACKNOWLEDGMENTS

We benefitted from discussions with M. C. Goorden, Ph. Jacquod, and H. Schomerus. This work was supported by the Dutch Science Foundation NWO/FOM. J.T. acknowledges the financial support provided through the European Community's Human Potential Programme under Contract No. HPRN-CT-2000-00144, Nanoscale Dynamics.

APPENDIX A: CLASSICAL MAP

Here we derive the classical map that is associated with the quantum mechanical Floquet operator of the kicked rotator with broken TRS. We consider the three-kick and one-kick representations separately.

1. Three-kick representation

We seek the classical limit of the Floquet operator (2.12). We consider the classical motion from θ_0 at $t=0$ to θ_T at $t=T$ (in units of τ_0). Intermediate values of the coordinate are denoted by θ_t, $t=0,1,\ldots,T$. The classical action $\mathcal{S}$ is the sum

$$\mathcal{S} = \sum_{t=0}^{T-1} S(\theta_{t+1}, \theta_t). \tag{A1}$$

Following the general method of Ref. 7 we derive

$$S(\theta', \theta) = S_c(\theta', \theta_2) + S_b(\theta_2, \theta_1) + S_a(\theta_1, \theta), \tag{A2}$$

$$S_a(\theta_1, \theta) = \tfrac{3}{2}(\theta_1 - \theta + 2\pi\sigma_{\theta_1})^2 - 6\pi\sigma_{p_1}\theta_1 + \gamma\cos(\theta_1) - \tfrac{1}{2}V(\theta), \tag{A3}$$

$$S_b(\theta_2, \theta_1) = \tfrac{3}{2}(\theta_2 - \theta_1 + 2\pi\sigma_{\theta_2})^2 - 6\pi\sigma_{p_2}\theta_2, \tag{A4}$$

$$S_c(\theta', \theta_2) = \tfrac{3}{2}(\theta' - \theta_2 + 2\pi\sigma_{\theta'})^2 - 6\pi\sigma_{p'}\theta' - \gamma\cos(\theta_2) - \tfrac{1}{2}V(\theta). \tag{A5}$$

The integers σ_θ, σ_p are the winding numbers of a classical trajectory on a torus with $\theta \in [0, 2\pi)$ and $p \in [0, 6\pi)$. The map equations are derived from

$$p_1 = \frac{\partial}{\partial \theta_1} S_a(\theta_1, \theta), \quad p = -\frac{\partial}{\partial \theta} S_a(\theta_1, \theta), \tag{A6}$$

$$p_2 = \frac{\partial}{\partial \theta_2} S_b(\theta_2, \theta_1), \quad p_1 = -\frac{\partial}{\partial \theta_1} S_b(\theta_2, \theta_1), \tag{A7}$$

$$p' = \frac{\partial}{\partial \theta'} S_c(\theta', \theta_2), \quad p_2 = -\frac{\partial}{\partial \theta_2} S_c(\theta', \theta_2). \tag{A8}$$

Equations (A6)–(A8) are equivalent to the following set of six equations that map initial coordinates (θ, p) onto final coordinates (θ', p') after one period:

$$\begin{cases} \theta_1 = \theta + p/3 - V'(\theta)/6 - 2\pi\sigma_{\theta_1}, \\ p_1 = p - \gamma\sin\theta_1 - V'(\theta)/2 - 6\pi\sigma_{p_1}, \end{cases} \tag{A9}$$

$$\begin{cases} \theta_2 = \theta_1 + p_1/3 - 2\pi\sigma_{\theta_2}, \\ p_2 = p_1 - 6\pi\sigma_{p_2}, \end{cases} \tag{A10}$$

$$\begin{cases} \theta' = \theta_2 + p_2/3 + \gamma\sin\theta_2/3 - 2\pi\sigma_{\theta'}, \\ p' = p_2 + \gamma\sin\theta_2 - V'(\theta')/2 - 6\pi\sigma_{p'}. \end{cases} \tag{A11}$$

We denote $V' = dV/d\theta$. Winding numbers of a trajectory on the torus in phase space (θ, p) are denoted by σ_θ, σ_p. These integers are determined by the requirement that $\theta, \theta_1, \theta_2, \theta' \in [0, 2\pi)$ and $p, p_1, p_2, p' \in [0, 6\pi)$. TRS for a classical map means that the point $(\theta', -p')$ maps to $(\theta, -p)$. This property is satisfied for $\gamma = 0$, but not for $\gamma \neq 0$. TRS is broken at the classical level in the three-kick model.

2. One-kick representation

We now seek the classical limit of the Floquet operator (2.14). The classical action S after one kick is

$$S(\theta', \theta) = \tfrac{1}{2}(\theta' - \theta + 2\pi\sigma_\theta)^2 - 2\pi\sigma_p\theta' + \delta(\theta' - \theta) + 2\pi\sigma\delta - \frac{1}{2}K[\cos(\theta + \phi) + \cos(\theta' + \phi)]. \tag{A12}$$

The map equations are derived from

$$p' = \frac{\partial}{\partial \theta'} S(\theta', \theta), \quad p = -\frac{\partial}{\partial \theta} S(\theta', \theta). \tag{A13}$$

The mapping of initial coordinates (θ, p) onto final ones (θ', p') after one kick is then

$$\begin{cases} \theta' = \theta + p + \dfrac{1}{2}K\sin(\theta+\phi) - \delta - 2\pi\sigma_\theta, \\ p' = p + \dfrac{1}{2}K[\sin(\theta+\phi) + \sin(\theta'+\phi)] - 2\pi\sigma_p. \end{cases} \tag{A14}$$

The constant $2\pi\sigma\delta$ in the action (A12), which has no dynamical effect in the classical limit, is determined by the integer σ. This is the winding number after the first half of the kick of the intermediate momentum $p_1=\theta'-\theta+\delta+\pi+2\pi\sigma\in[0,2\pi]$.

The canonical transformation $p-\delta\to\tilde{p}$, $\theta+\phi\to\tilde{\theta}$ brings the map to an equivalent form

$$\begin{cases} \tilde{\theta}' = \tilde{\theta} + \tilde{p} + \frac{1}{2}K\sin\tilde{\theta} - 2\pi\sigma_\theta, \\ \tilde{p}' = \tilde{p} + \frac{1}{2}K(\sin\tilde{\theta} + \sin\tilde{\theta}') - 2\pi\sigma_p. \end{cases} \tag{A15}$$

This form is manifestly invariant under the transformation that maps $(\tilde{\theta}',-\tilde{p}')$ onto $(\tilde{\theta},-\tilde{p})$ for any value of ϕ and δ. Hence TRS is not broken at the classical level in the one-kick model.

APPENDIX B: DERIVATION OF EQS. (3.8) AND (3.9)

In the large-K limit the level curvature in the kicked rotator can be related to the level curvature in the Pandey-Mehta Hamiltonian. This leads to the relations (3.8) and (3.9) between the TRS breaking parameters γ (three-kick model) and δ (one-kick model), on the one hand, and the Pandey-Mehta parameter α, on the other hand.

Perturbation theory for eigenphases $\phi_i(\delta\gamma)$ of a unitary matrix $\mathcal{F}(\delta\gamma)$ gives the series expansion

$$\phi_i(\delta\gamma) = \phi_i + W_{ii}\delta\gamma + \tfrac{1}{2}\sum_{j\neq i}|W_{ij}|^2(\delta\gamma)^2\cot(\phi_i-\phi_j)/2 + \tfrac{1}{2}V_{ii}(\delta\gamma)^2. \tag{B1}$$

Here ϕ_i denotes an eigenphase of $\mathcal{F}(0)=U\,\mathrm{diag}(e^{i\phi_1},\ldots,e^{i\phi_M})U^\dagger$. The Hermitian matrices W and V are defined by $W=U(-i\mathcal{F}^\dagger\partial_\gamma\mathcal{F}|_{\gamma=0})U^\dagger$, $V=\partial_\gamma W|_{\gamma=0}$. Due to reciprocity of $\mathcal{F}$ we find $W_{ii}=0$. For the three-kick model (2.12) the operators W, V are

$$W = \frac{M}{6\pi}UX^\dagger\Pi^\dagger Y^\dagger\Pi^\dagger(-C\Pi+\Pi C)Y\Pi XU^\dagger, \tag{B2}$$

$$V = i\left(\frac{M}{6\pi}\right)^2 UX^\dagger\Pi^\dagger Y^\dagger(C\Pi^\dagger C\Pi - \Pi^\dagger C\Pi C)Y\Pi XU^\dagger, \tag{B3}$$

where $C_{mm'}=\delta_{mm'}\cos(2\pi m/M)$. We assume that for strongly chaotic systems ($K\gg1$) the matrix elements W_{ij} and V_{ii} are random Gaussian numbers independent of the eigenphases. Average diagonal elements calculated in the three kick model at $\gamma=0$ are $\langle V_{ii}\rangle=\mathrm{Tr}\,V/M=0$ and $\langle W_{ii}\rangle=\mathrm{Tr}W/M=0$. The variance of the off-diagonal elements is $\langle|W_{ij}|^2\rangle=\mathrm{Tr}\,WW^\dagger/M^2=M/(6\pi)^2$.

For the one-kick model (2.14) the operators W,V are

$$W = UX^\dagger\tilde{U}^\dagger D\tilde{U}XU^\dagger, \quad V=-\frac{1}{2\pi}M, \tag{B4}$$

with $D_{mm'}=\delta_{mm'}(m+1/2-M/2-\delta M/2\pi)$. Average diagonal elements at $\delta=0$ are $\langle V_{ii}\rangle=\mathrm{Tr}\,V/M=-M/2\pi$ and $\langle W_{ii}\rangle=\mathrm{Tr}\,W/M=0$. The variance of the off-diagonal elements is $\langle|W_{ij}|^2\rangle=\mathrm{Tr}\,WW^\dagger/M^2=M/12$.

For $K\gg1$ the eigenphases ϕ_i are distributed randomly in the circular ensemble, which is locally equivalent to the Gaussian ensemble.[1] We expand Eq. (B1) for small eigenphases difference, compare with Eq. (3.2), and substitute the variances of matrix elements calculated above. For the one-kick model we drop terms with V_{ii} as they are of order $1/M$. We finally arrive at Eqs. (3.8) and (3.9).

The explicit formula for the Pandey-Mehta parameter α describing the kicked rotator at large K is

$$\alpha\sqrt{M_H} = \frac{\gamma M^{3/2}}{12\pi} \tag{B5}$$

for the three-kick model. The corresponding formula for the one-kick model is

$$\alpha\sqrt{M_H} = \frac{\delta M^{3/2}}{4\sqrt{3}}. \tag{B6}$$

APPENDIX C: SEMICLASSICAL DERIVATION OF THE WEAK LOCALIZATION PEAK

We present a semiclassical derivation of the weak localization peak, adopting the method of Ref. 8 to the case of the kicked rotator. The method cannot be used to determine the amplitude $\delta G(0)$, but we use it for the crossover scale. This serves as an independent check for the scaling predicted by RMT.

The action difference in the three-kick model for a pair of trajectories related by TRS is calculated as follows. The action $\mathcal{S}_0$ for a trajectory with initial coordinate θ_0 and final coordinate θ_T at $\gamma=0$ is compared with the action $\mathcal{S}$ for a trajectory with the same initial and final coordinates, but at small γ. The result of linear expansion in γ is

$$\Delta S = \mathcal{S}-\mathcal{S}_0 = \gamma\sum_t[\cos\theta_1(t)-\cos\theta_2(t)], \tag{C1}$$

where periods are numbered by $t=0,1,\ldots,T-1$ and $\theta_1(t)$, $\theta_2(t)$ denote the coordinate of the particle when TRS-breaking kicks are applied.

The weak localization correction is

$$\delta G \propto \langle\exp(2i\Delta S/\hbar_{\mathrm{eff}})\rangle, \tag{C2}$$

where the average is taken with respect to all trajectories connecting initial to final coordinates. Approximating the distribution of the phase difference ΔS for a single step by a Gaussian, and taking the continuum limit of exponential dwell-time probability $P(t)\propto e^{-t/\tau_D}$, we derive

$$\delta G \propto [1 + (M\gamma/\gamma^*)^2]^{-1}, \quad (\gamma^*)^2 = 2\hbar_{\rm eff}^2/(\tau_D \nu), \quad \text{(C3)}$$

with ν being the variance of $\Delta S/\gamma$ for a single step. The result $\nu=1$ for large K (and large τ_D) is obtained by averaging over random initial points in the whole phase space. We thus find Eq. (4.2), the same result as the one obtained in RMT.

The action difference for a pair of symmetry related trajectories in the one-kick model is

$$\Delta S = \mathcal{S} - \mathcal{S}_0 = \delta \sum_t [\theta'(t) - \theta(t) + 2\pi\sigma(t)], \quad \text{(C4)}$$

to linear order in δ. This leads to

$$\delta G \propto [1 + (M\delta/\delta^*)^2]^{-1}, \quad (\delta^*)^2 = 2\hbar_{\rm eff}^2/(\tau_D \nu). \quad \text{(C5)}$$

By averaging over random initial points in the whole phase space for large K and τ_D we find $\nu = 4\pi^2/3$. Hence we obtain Eq. (4.3), the result of RMT.

[1] F. Haake, *Quantum Signatures of Chaos* (Springer, Berlin, 1992).
[2] C. W. J. Beenakker, Rev. Mod. Phys. **69**, 731 (1997).
[3] T. Guhr, A. Müller-Groeling, and H. A. Weidenmüller, Phys. Rep. **299**, 190 (1998).
[4] Y. Alhassid, Rev. Mod. Phys. **72**, 895 (2000).
[5] O. Bohigas, M. G. Giannoni, A. M. Ozorio de Almeida, and C. Schmit, Nonlinearity **8**, 203 (1995).
[6] Z. D. Yan and R. Harris, Europhys. Lett. **32**, 437 (1995).
[7] P. Shukla and A. Pandey, Nonlinearity **10**, 979 (1997).
[8] H. U. Baranger, R. A. Jalabert, and A. D. Stone, Phys. Rev. Lett. **70**, 3876 (1993); Chaos **3**, 665 (1993).
[9] Z. Pluhar, H. A. Weidenmüller, J. A. Zuk, and C. H. Lewenkopf, Phys. Rev. Lett. **73**, 2115 (1994).
[10] K. B. Efetov, Phys. Rev. Lett. **74**, 2299 (1995).
[11] K. Frahm, Europhys. Lett. **30**, 457 (1995); K. Frahm and J.-L. Pichard, J. Phys. I **5**, 847 (1995).
[12] Y. V. Fyodorov and H.-J. Sommers, JETP Lett. **72**, 422 (2000).
[13] A. Ossipov, T. Kottos, and T. Geisel, Europhys. Lett. **62**, 719 (2003).
[14] Ph. Jacquod, H. Schomerus, and C. W. J. Beenakker, Phys. Rev. Lett. **90**, 207004 (2003).
[15] J. Tworzydło, A. Tajic, H. Schomerus, and C. W. J. Beenakker, Phys. Rev. B **68**, 115313 (2003).
[16] F. M. Izrailev, Phys. Rev. Lett. **56**, 541 (1986).
[17] F. M. Izrailev, Phys. Rep. **196**, 299 (1990).
[18] R. Blümel and U. Smilansky, Phys. Rev. Lett. **69**, 217 (1992).
[19] M. Thaha, R. Blümel, and U. Smilansky, Phys. Rev. E **48**, 1764 (1993).
[20] T. O. de Carvalho, J. P. Keating, and J. M. Robbins, J. Phys. A **31**, 5631 (1998).
[21] T. Dittrich, R. Ketzmeric, M.-F. Otto, and H. Schanz, Ann. Phys. (Leipzig) **9**, 755 (2000).
[22] P. H. Jones, M. Goonasekera, H. E. Saunders-Singer, and D. R. Meacher, quant-ph/0309149.
[23] T. Jonckheere, M. R. Isherwood, and T. S. Monteiro, Phys. Rev. Lett. **91**, 253003 (2003).
[24] G. Casati, R. Graham, I. Guarneri, and F. M. Izrailev, Phys. Lett. A **190**, 159 (1994).
[25] T. Kottos, A. Ossipov, and T. Geisel, Phys. Rev. E **68**, 066215 (2003).
[26] P. Shukla, Phys. Rev. E **53**, 1362 (1996).
[27] M. C. Goorden and Ph. Jacquod (private communication).
[28] M. L. Mehta and A. Pandey, J. Phys. A **16**, 2655 (1983).
[29] J. Tworzydło, A. Tajic, and C. W. J. Beenakker, Phys. Rev. B **69**, 165318 (2004).
[30] Ph. Jacquod and E. V. Sukhorukov, Phys. Rev. Lett. **92**, 116801 (2004).
[31] P. G. Silvestrov, M. C. Goorden, and C. W. J. Beenakker, Phys. Rev. Lett. **90**, 116801 (2003); Phys. Rev. B **67**, 241301 (2003).
[32] I. L. Aleiner and A. I. Larkin, Phys. Rev. B **54**, 14 423 (1996).
[33] I. Adagideli, Phys. Rev. B **68**, 233308 (2003).